

# Encapsulation of the Ethylene Inhibitor 1-Methylcyclopropene by Cucurbit[6]uril

Quan Zhang, Zeng Zhen, Hong Jiang,\* Xue-Gang Li, and Jun-An Liu

Department of Chemistry, Huazhong Agricultural University, Wuhan 430070, China

**ABSTRACT:** 1-Methylcyclopropene (1-MCP) is an excellent safe and commercially available ethylene antagonist for the preservation of horticultural products. However 1-MCP has to be stored in absorbents due to its gaseous and unstable characteristics. In this paper cucurbit[6]uril (CB[6]) was used as the absorbent to encapsulate 1-MCP, and the resultant inclusion complex was characterized by IR, powder X-ray diffraction, thermal analysis, and fluorescent spectra. The effects of encapsulation conditions on the formation of inclusion complex were also investigated. The amount of 1-MCP encapsulated by CB[6] was about 4.5% by weight when the initial concentration of 1-MCP, encapsulation temperature, CB[6] concentration, and encapsulation time were set at 75 mL/L, 20 °C, 30 mM, and 8 h, respectively. Furthermore, the release of 1-MCP from the complex can be realized with different solutions such as sodium bicarbonate, benzoic acid, and distilled water. CB[6] can be used as an excellent absorbent for encapsulation of 1-MCP.

**KEYWORDS:** 1-methylcyclopropene, cucurbituril, inclusion complex, kinetic study

## INTRODUCTION

As a plant growth regulator, ethylene can mediate a variety of growth phenomena including ripening and senescence in plants.<sup>1</sup> Accordingly, ethylene can profoundly affect the quality of harvested products, which may be beneficial or deleterious depending on the product, ripening stage, and desired use. However, avoiding exposure to ethylene and/or attempting to diminish ethylene biosynthesis and action during the ripening, harvest, storage, transport, and handling of horticultural products is more frequently desired.<sup>2</sup> Thus, ethylene antagonists are of tremendous commercial value in the horticultural industry. The most prominent of currently known ethylene antagonists are 1-alkylcyclopropenes, which are believed to interact with ethylene receptors and thereby prevent ethylene-dependent responses. Among them, 1-methylcyclopropene (1-MCP) has now been approved commercially for application on horticultural products because of its nontoxic mode of action,<sup>3</sup> negligible residue, and being active at very low concentrations.<sup>4–6</sup> The use of 1-MCP on fruits and vegetables now has been extensively reviewed in the literature.<sup>7–10</sup> However, under normal environmental conditions, 1-MCP is gaseous and chemically unstable. Furthermore, it presents an explosive hazard when compressed. To solve these problems, several methods have been developed to incorporate 1-MCP into molecular encapsulation agents, such as molecular sieves,<sup>11</sup> modified starch,<sup>12</sup> sawdust,<sup>13</sup> and cyclodextrin,<sup>14</sup> of which  $\alpha$ -cyclodextrin ( $\alpha$ -CD) is the most preferred one.<sup>15,16</sup> 1-MCP can be easily released as a gas when the 1-MCP/ $\alpha$ -CD inclusion complex powder is dissolved in water. Now 1-MCP/ $\alpha$ -CD is commercially available under the trade name SmartFresh. However,  $\alpha$ -CD was not cheap enough for its popularity. 1-MCP can be released from a 1-MCP/ $\alpha$ -cyclodextrin complex after the addition of water, but the release rate of 1-MCP cannot be realized controllably. Therefore, it is still meaningful to explore new materials to encapsulate 1-MCP.

Cucurbit[*n*]urils (CB[*n*], *n* is the number of glycoluril units) are barrel-like macrocyclic molecules, which are prepared from the cheap starting materials glycoluril and formalin (Figure 1). Because they have cavities to host small molecules, the popularity of CB[*n*] has grown substantially in recent years.<sup>17–20</sup> The cavity size of CB[6] is similar to that of  $\alpha$ -CD.<sup>21–23</sup> CB[6] can form stable inclusion complexes with alkylammonium ions,<sup>24</sup> short polypeptides,<sup>25</sup> Et<sub>2</sub>O,<sup>26</sup> metal cations,<sup>27</sup> and some small-molecule gases.<sup>28</sup> The similar cavity characteristics between CB[6] and  $\alpha$ -CD inspired us to explore the possibility of using CB[6] as potential absorbent for 1-MCP. Herein the preparation and characterization of 1-MCP/CB[6] inclusion complex is reported.

## MATERIALS AND METHODS

**Materials.** All of the chemicals used were of reagent grade unless otherwise indicated. 3-Chloro-2-methylpropene (98%) and phenyl lithium were purchased from Sinopharm Chemical Reagent Co. Ltd. Distilled water was used throughout the entire experiment. CB[6] was prepared in the laboratory by acidic condensation of glycoluril with formaldehyde.<sup>18,29</sup> Briefly, a mixture of glycoluril (8 g, 0.078 mol), formaldehyde (3.45 g, 0.115 mol), and 9 M hydrochloric acid (20 mL) was heated at 60 °C for 1 h. Then, the concentrated sulfuric acid was added and was heated at 80 °C for 48 h. After the reaction mixture was poured into water, the precipitate was filtered and washed to neutral by water. The CB[6] powder was dried in vacuo at 70 °C for 24 h before use.

**1-MCP Synthesis.** 1-MCP was produced according to the literature.<sup>30,31</sup> Briefly, 3.6 mL (0.03 mol) of 3-chloro-2-methylpropene (98%) in 30 mL of ether (dried over sodium) was added dropwise to 5 g (0.06 mol) of a slurry of phenyl lithium in 30 mL of ether at room temperature. A slow stream of nitrogen gas was passed over the reaction mixture. When the addition of 3-chloro-2-methylpropene was finished

**Received:** May 17, 2011

**Revised:** September 2, 2011

**Accepted:** September 6, 2011

**Published:** September 06, 2011

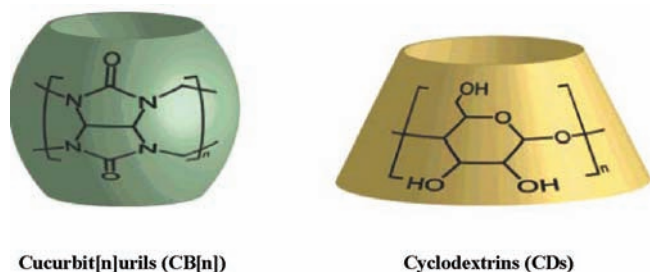


**Figure 1.** Structures and schematic representations of CB and CD.

(approximately 1 h), the reaction was continued for 2 h with stirring and the lithium salt of 1-MCP was formed as a suspension in ether. After reaction, vacuum was pulled to about 0.1 kPa to eliminate volatile impurities, and then the product was stored at  $-4^{\circ}\text{C}$  until use. 1-MCP can be easily synthesized by the direct reaction of lithium salt of 1-MCP with water.

**Quantification of 1-MCP.** Quantities of 1-MCP were measured on a Fuli gas chromatograph (Fuli Corp., Zhejiang, China) fitted with a capillary column and a flame ionization detector. The injection pot and detector temperatures were set at 110 and  $200^{\circ}\text{C}$ , respectively. The column temperature was  $60^{\circ}\text{C}$  with a hold time of 3 min. Quantification of 1-MCP was accomplished using an external standard method. The isobutylene gas standard of  $100\ \mu\text{L/L}$  concentration was used. It was presumed that quantities of 1-MCP had a response factor similar to that of isobutylene.

**Preparation of 1-MCP/CB[6] Inclusion Complex.** The inclusion of 1-MCP with CB[6] was carried out in a closed agitated vessel. A 250 mL glass bottle with a modified screw cap was used as the encapsulation vessel. A CB[6] suspension of 30 mM was prepared in the encapsulation vessel, based on 50 mL of distilled water. Another 250 mL glass bottle was used as the reaction vessel. The initial head space concentration of 1-MCP was about 75 mL/L by the reaction of lithium salt of 1-MCP with water in the reaction vessel. The encapsulation vessel and the reaction vessel were connected to each other with a tube. First, vacuum was pulled to about 0.1 kPa in the encapsulation vessel. Then 5 mL of distilled water was injected into the reaction vessel containing lithium salt of 1-MCP to produce 1-MCP, which was transferred to the encapsulation vessel by pressure gradient. During the encapsulation process, nitrogen was added slowly into the reaction vessel to create a pressure gradient. This procedure was repeated until the pressure of both vessels reached the atmospheric value. Encapsulation temperatures were at  $20^{\circ}\text{C}$ , and the encapsulation time was about 8 h. At the end of the process, the 1-MCP/CB[6] inclusion complex was collected by filtration and then dried in vacuo for 10 h at  $30^{\circ}\text{C}$  before further analyses and stored in a desiccator.

**Fourier Transform Infrared Spectroscopy (FT-IR).** FT-IR spectra were recorded from  $4000$  to  $400\ \text{cm}^{-1}$ , using a Fourier transform model Nexus 870 infrared spectrometer (Thermo Nicolet Corp.) on samples prepared as KBr disks. The FT-IR spectra of CB[6] and the 1-MCP/CB[6] inclusion complex are shown in Figure 2.

**Powder X-ray Diffractometry (PXRD).** PXRD profiles of both CB[6] and the 1-MCP/CB[6] complex were recorded on the Bruker D8 Advance X-ray diffractometer (Bruker Corp.). Measurements were performed using Cu K $\alpha$  radiation ( $\lambda = 1.5406\ \text{\AA}$ ) operating at 40 kV and 40 mA. Samples were scanned at a scanning speed of  $10^{\circ}/\text{min}$  over a diffraction angular range of  $3^{\circ} < 2\theta < 30^{\circ}$ . The divergence slit, receiving slit, and time constant were set at  $0.02^{\circ}$ , 0.3 mm, and 1 s, respectively.

**Thermal Analysis of the Inclusion Complex.** Thermogravimetric (TG) curves were recorded on a Netzsch TG209C (Netzsch Corp.) equipped with Proteus Analysis software. Samples of 10 mg were weighed into aluminum pans for analysis at a heating rate of  $5^{\circ}\text{C}/\text{min}$  from 30 to  $450^{\circ}\text{C}$  under a nitrogen flow at  $50\ \text{mL}/\text{min}$ .

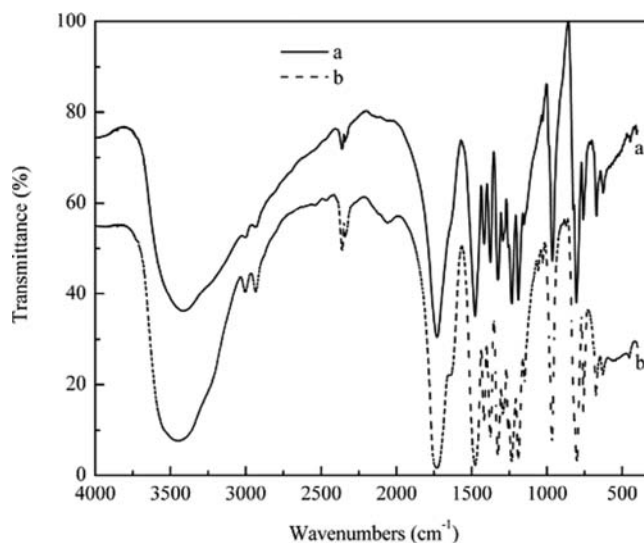


**Figure 2.** FT-IR absorption spectrum of (a) CB[6] only and (b) the 1-MCP/CB[6] inclusion complex, which was prepared with the initial concentration of 1-MCP, encapsulation temperature, CB[6] concentration, and encapsulation time set at 75 mL/L,  $20^{\circ}\text{C}$ , 30 mM, and 8 h, respectively.

Differential scanning calorimetry (DSC) curves were recorded on a Netzsch DSC204 equipped with Proteus Analysis software. Samples of 10 mg were weighed into aluminum pans for analysis at a heating rate of  $5^{\circ}\text{C}/\text{min}$  from 30 to  $500^{\circ}\text{C}$  under a nitrogen flow at  $50\ \text{mL}/\text{min}$ .

**Fluorescence Spectra (FL).** All fluorescence spectra were recorded by an RF-5301PC fluorescence spectrometer (Shimadzu) equipped with a 20 kW xenon discharge lamp as a light source. The excitation wavelength, slit width of excitation, and slit width of emission were set at 288, 10, and 20 nm, respectively. The fluorescence of CB[6] and its inclusion complex were recorded immediately after its saturated solutions were prepared in distilled water.

**Determination of the 1-MCP Inclusion Ratio in 1-MCP/CB[6] Inclusion Complexes.** The inclusion ratio of 1-MCP/CB[6] inclusion complex is defined as the mass ratio of 1-MCP to CB[6] in the inclusion complex. The inclusion ratio of the inclusion complex was calculated from the TG data.

**Effects of Encapsulation Conditions on the 1-MCP Retention.** Encapsulation conditions on the inclusion of 1-MCP were investigated and assessed as the retention value, which was calculated as

$$r = C_{1\text{-MCP}}/C_0 \quad (2-1)$$

where  $C_{1\text{-MCP}}$  is the 1-MCP head space concentration and  $C_0$  is the initial head space value of 1-MCP.

The initial concentration of 1-MCP, CB[6] concentration, and encapsulation temperature were varied to investigate the effect of encapsulation conditions on the 1-MCP retention.

**Effect of Initial Concentration of 1-MCP on 1-MCP Retention.** To evaluate the effect of the initial concentration of 1-MCP on 1-MCP retention, the initial concentration of 1-MCP was tested at 50, 75, and  $100\ \text{mL}/\text{L}$ . Encapsulation temperature, CB[6] concentration, and encapsulation time were set at  $20^{\circ}\text{C}$ , 30 mM, and 8 h, respectively.

**Effect of CB[6] Concentration on 1-MCP Retention.** The CB[6] concentration was tested at 50, 30, and 20 mM to evaluate the effect of CB[6] concentration on 1-MCP retention. The initial concentration of 1-MCP, temperature, and encapsulation time were  $75\ \text{mL}/\text{L}$ ,  $20^{\circ}\text{C}$ , and 8 h, respectively.

**Effect of Encapsulation Temperature on 1-MCP Retention.** To evaluate the effect of encapsulation temperature on 1-MCP retention, experiments

within the range 15–25 °C were carried out. The initial 1-MCP head space concentration, CB[6] concentration, and encapsulation time were set at 75 mL/L, 30 mM, and 8 h, respectively.

**Kinetic Model Fitting.** To investigate the possible kinetic model, two models have been checked for the possible experimental data fitting. One is a pseudo-first-order kinetic model, and the other is a pseudo-second-order kinetic model.

$Q$  is the sorption amount, which is calculated using the mass balance

$$Q = M_{1-MCP}V(1-r)C_0/22.4m \quad (2-2)$$

where 22.4 (L/mol) is the molar volume of gas,  $M_{1-MCP}$  is the molar mass of 1-MCP,  $m$  (g) is the amount of CB[6],  $V$  is the net volume of the reaction equipment,  $C_0$  is the initial concentration of 1-MCP, and  $r$  is the 1-MCP retention at time  $t$  (min).

The pseudo-first-order equation is commonly represented by<sup>32</sup>

$$\ln(Q_e - Q_t) = \ln Q_e - k_1 t \quad (2-3)$$

where  $k_1$  (1/min) is the pseudo-first-order adsorption rate constant,  $Q_t$  is the amount adsorbed at time  $t$  (min), and  $Q_e$  denotes the amount adsorbed at equilibrium;  $Q_t$  and  $Q_e$  are both in mg/g. The plot of  $\ln(Q_e - Q_t)$  versus  $t$  gives the  $k_1$  and  $Q_e$  values.

The pseudo-second-order equation is applied in the form<sup>32</sup>

$$\frac{t}{Q_t} = \frac{1}{k_2 Q_e^2} + \frac{1}{Q_e} t \quad (2-4)$$

where  $k_2$  (g/(mg min)) is the rate constant and  $Q_e$  is the equation adsorption capacity (mg/g).

**Release of 1-MCP from the Inclusion Complex.** The method was as follows: 0.1 g of inclusion complex was weighed out in a 25 mL vial, and then 1 mL of 3% NaHCO<sub>3</sub> solution, benzoic acid solution, or distilled water was injected into the vial through a butyl rubber stopper. Then, 2 mL sample from the headspace of vial was injected into the gas chromatograph (Fuli Analytical Instrument Co., Ltd.) per 20 min to determine the concentration of 1-MCP in the vial. The detailed quantification method was the same as in the above section Quantification of 1-MCP.

**Statistical Analysis.** SPSS 17.0 software (SPSS Inc., Chicago, IL) was used to test the significance using the general linear model to determine the treatment and interaction effects and Tukey's test for comparing the levels. Three replicates per treatment were used in all experiments. Data were tested for multiple comparisons by analysis of variance (ANOVA) with least significant difference (LSD) between averages determined at the 5% level.

## RESULTS AND DISCUSSION

**FT-IR, X-RD, TG, DSC, and FL Analysis.** The FT-IR spectra of CB[6] and the 1-MCP/CB[6] inclusion complex are shown in Figure 2. The broad band of CB[6] (a) at 3428 cm<sup>-1</sup> was due to the stretching mode of the O–H groups. The bands at 3002 and 1481 cm<sup>-1</sup> suggest the presence of a –CH<sub>2</sub>– group. The strong peak at 1700 cm<sup>-1</sup> band is caused by the C=O stretching band of the carboxyl group.<sup>33,34</sup> The spectrum of the inclusion complex (b) is similar to that of CB[6], but the weak peak at 1681 cm<sup>-1</sup> implies the presence of a carbon–carbon double bond of 1-MCP,<sup>35</sup> indicating the presence of 1-MCP adsorbed in CB[6]. It also suggesting that 1-MCP is encapsulated within CB[6]'s cavity rather than being chemically bonded to it.

The PXRD patterns of CB[6] and the 1-MCP/CB[6] inclusion complex are given in Figure 3. The characteristic peaks of CB[6] (Figure 3a) were at  $2\theta = 9.1^\circ, 14.5^\circ, 15.6^\circ, 18.1^\circ, 21.3^\circ,$  and  $23.9^\circ$ .<sup>36</sup> It was shown that some of the characteristic peaks of CB[6] decreased in intensity or even disappeared in the 1-MCP/CB[6] inclusion complex (Figure 3b); moreover, some new peaks were

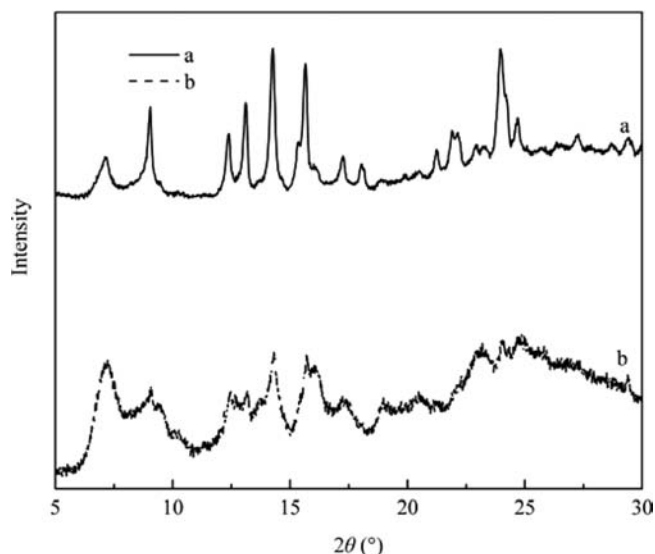


**Figure 3.** Powder X-ray diffraction patterns of (a) CB[6] only and (b) the 1-MCP/CB[6] inclusion complex, which was prepared as in Figure 2.

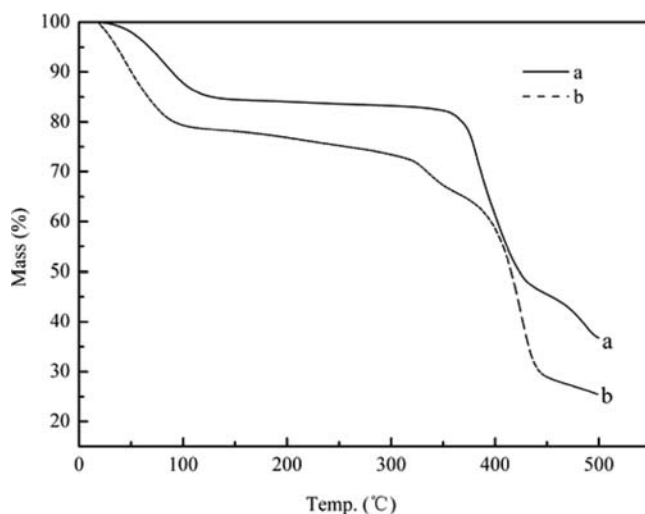


**Figure 4.** TG curves of (a) CB[6] only and (b) the 1-MCP/CB[6] inclusion complex, which was prepared as in Figure 2.

found at  $2\theta = 9.4^\circ, 16.1^\circ, 20.5^\circ,$  and  $23.1^\circ$ . These indicated the ordered structure of the crystalline region on the CB[6] was disrupted. The peaks in PXRD were broadened after complexation with 1-MCP, further demonstrating the crystallinity of CB[6] decreased after encapsulation of 1-MCP.

Figure 4 represents the TG curves of CB[6] and 1-MCP/CB[6]. It appeared that a slow weightlessness was produced at the beginning in CB[6] (a), with a  $4.5 \pm 0.5\%$  mass loss from 40 to 110 °C, which might be the amount of water absorbed by dehydration.<sup>35,36</sup> The weightlessness ladder for 1-MCP/CB[6] (b) was about  $9 \pm 0.3\%$  mass loss in the similar temperature region. This additional 4.5% mass loss should result from the release of 1-MCP from CB[6]'s cavity. A larger weightlessness ladder appeared because of the self-decomposition of CB[6] after 350 °C in comparison to 1-MCP/CB[6] after 320 °C; thus, the stability of CB[6] decreased after encapsulation of 1-MCP,

which is consistent with the deduction of the crystallinity of CB[6] in the PXRD.

Figure 5 represents the DSC curves of CB[6] and 1-MCP/CB[6], recorded at the heating rate of 5 °C/min. CB[6] (a) had a

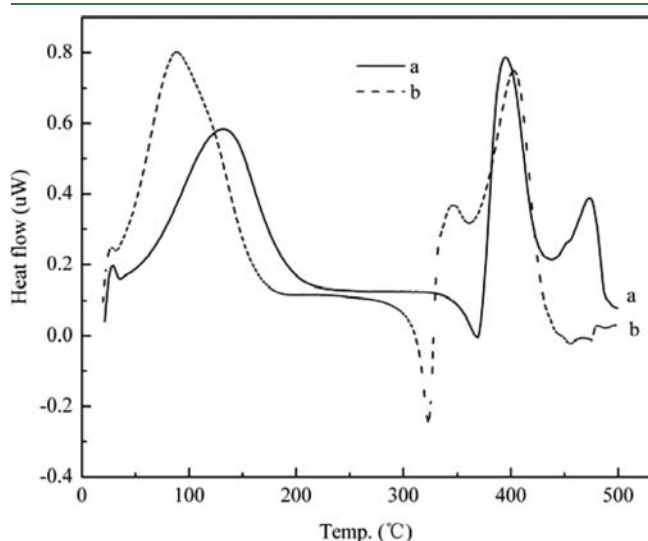


**Figure 5.** DSC curves of (a) CB[6] only and (b) the 1-MCP/CB[6] inclusion complex, which was prepared as in Figure 2.

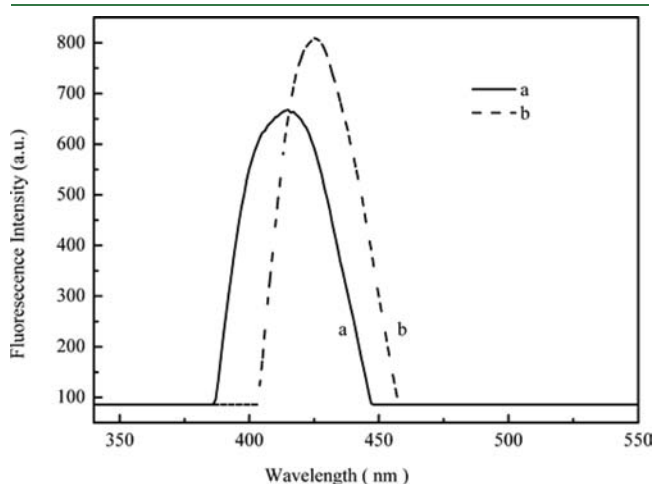


**Figure 6.** Fluorescence spectrum curves of (a) CB[6] only and (b) the 1-MCP/CB[6] inclusion complex, which was prepared as in Figure 2.

wide dehydration phase from 30 to 130 °C as endothermic processes with one sharp peak at 120 °C, but after absorption of 1-MCP, the endothermic peak appeared at 100 °C, indicating the stability decreased. Furthermore, the intensity of 1-MCP/CB[6]'s endothermic peak at 100 °C was larger than that of uncomplexed CB[6] at 120 °C in DSC, which may be ascribed to the additional endothermic release of 1-MCP along with the dehydration for the 1-MCP/CB[6] inclusion complex.

Figure 6 represents the fluorescence spectrum curves of CB[6] and 1-MCP/CB[6]. The fluorescence emission peak of CB[6] is 417 nm (Figure 6a); a red shift on the emission spectra maximum can be observed from 417 to 429 nm for 1-MCP/CB[6] (Figure 6b). This may be because the hydrophobic cavity of CB[6] was occupied by 1-MCP, leading to the increased fluorescence intensity and the red shift of the maximum emission peak.<sup>37</sup>

On the whole, both the weak carbon–carbon double bond peak at 1681  $\text{cm}^{-1}$  in FTIR and the red shift on the emission spectra in fluorescence spectrum curves proved the formation of new product. The encapsulation of 1-MCP was also demonstrated by the disrupted crystalline of CB[6] in PXRD curves, which is consistent with the change in the endothermic peak place and peak strength of DSC curves. In TG the additional 4.5% mass loss further indicated the amount of 1-MCP absorbed by CB[6]. In all, FTIR, FL, XRD, TG, and DSC from different aspects demonstrated the successful preparation of the 1-MCP/CB[6] inclusion complex.

**Effect of Initial Concentration of 1-MCP on 1-MCP Retention.** The effect of the initial concentration of 1-MCP on the 1-MCP retention is illustrated in Figure 7a. As the initial concentration of 1-MCP increased from 50 to 100 mL/L, the 1-MCP retention increased from 0.14 to 0.31. At the beginning of the encapsulation reaction, the 1-MCP head space concentration dropped at a higher rate, and finally the 1-MCP retention almost kept different constant values depending on the different initial concentration of 1-MCP. We can also see that the higher the initial concentration of 1-MCP, the less time to reach equilibrium.

**Effect of CB[6] Concentration on 1-MCP Retention.** Figure 7b shows the effect of CB[6] concentration on 1-MCP retention. According to Figure 7b, when the CB[6] concentration rose from 20 to 50 mM, the 1-MCP retention decreased, and the 1-MCP retention almost kept a stable value at last.

**Effect of Encapsulation Temperature on 1-MCP Retention.** The results are shown in Figure 7c. The 1-MCP retention increased when the reaction temperature changed from 15 to 25 °C. As the reaction temperature rose, the solubility of 1-MCP in the CB[6] solution decreased and accordingly went against the

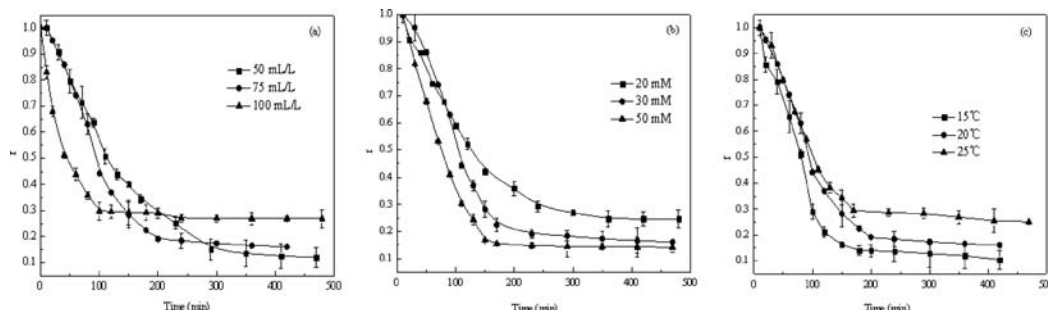


**Figure 7.** Effects of the initial concentration of 1-MCP (a), the CB[6] concentration (b), and encapsulation temperature (c) on 1-MCP retention. (a) The encapsulation temperature, the CB[6] concentration, and encapsulation time were 20 °C, 30 mM, and 8 h, respectively. (b) The initial concentration of 1-MCP, the temperature, and encapsulation time were 75 mL/L, 20 °C, and 8 h, respectively. (c) The initial 1-MCP head space concentration, CB[6] concentration, and encapsulation time were 75 mL/L, 30 mM, and 8 h, respectively. Vertical bars represent  $\pm 1$  standard deviation ( $n = 3$ ).

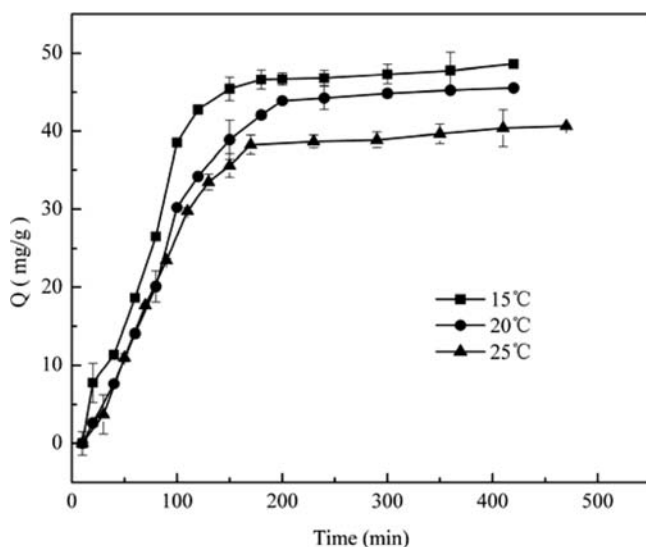


**Figure 8.** Adsorption kinetics of 1-MCP by CB[6] at various temperatures. The initial concentration of 1-MCP, CB[6] dose, and encapsulation time were 75 mL/L, 1.5 g (30 mM), and 8 h, respectively, for various temperatures. Vertical bars represent  $\pm 1$  standard deviation ( $n = 3$ ).

adsorption, so the 1-MCP retention increased. The optimal encapsulation temperature was 15 °C; however, for convenience, the preparation of the inclusion complex was set at 20 °C. Temperatures lower than 15 °C were not tested because the boiling point of 1-MCP is around 10 °C.<sup>38</sup>

**Absorption Kinetics.** As shown in Figure 8, absorption seems to occur in two steps; the first step involves rapid 1-MCP absorption, and then the sorption equilibrium is attained. To evaluate the kinetic mechanism that controls the adsorption process, two equations (i.e., pseudo-first-order equation, and pseudo-second-order equation) were tested to interpret the experimental data. The fitting results for the pseudo-first-order equation and pseudo-second-order equation are illustrated in Figures 9 and 10, and the related kinetic parameters are summarized in Table 1. On the basis of the obtained correlation coefficients ( $R^2$ ) from Table 1, the experimental data conformed neither to the pseudo-first-order equation nor to the pseudo-second-order equation.<sup>32</sup>

**Release of 1-MCP from 1-MCP/CB[6] Inclusion Complex.** The release of 1-MCP from the 1-MCP/CB[6] inclusion complex in different solutions, such as benzoic acid, sodium bicarbonate, and distilled water, was investigated. Benzoic acid, sodium bicarbonate, and distilled water were chosen as the releasing media on the basis of the following facts: These materials are nontoxic and easily available in our daily life. Moreover, they are the typical representatives for acid, alkali, and neutral media simulating living environments of horticultural crops. Gas chromatography was employed for the quantification of the 1-MCP released. It showed that the released 1-MCP immediately reached the concentration peak after only 10 min in sodium bicarbonate solution (Figure 11a), whereas for the benzoic solution (Figure 11b), it took about 90 min to arrive at the largest concentration. As for distilled water (Figure 11c) the largest concentration of released 1-MCP has not been achieved even after 2 h. The different release characteristics of 1-MCP at various conditions may be beneficial for the controlled release of

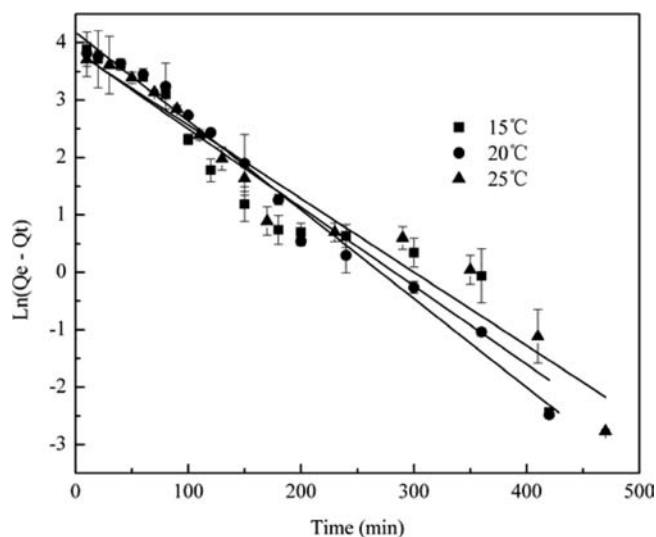


**Figure 9.** Fitting of pseudo-first-order equation at various temperatures. Vertical bars represent  $\pm 1$  standard deviation ( $n = 3$ ).

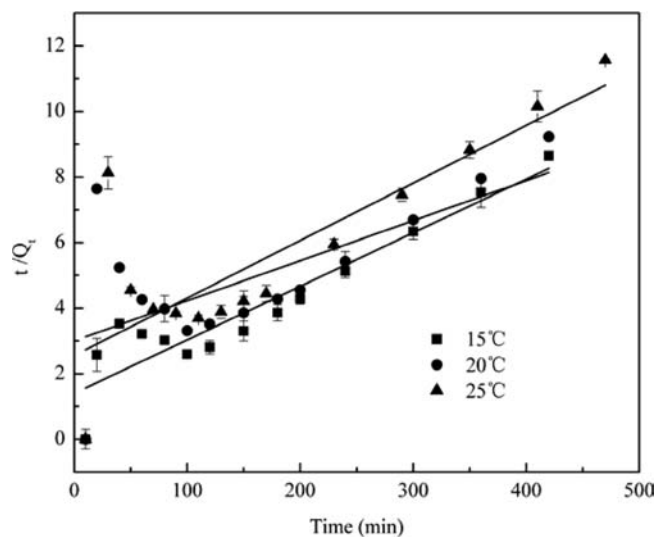


**Figure 10.** Fitting of pseudo-second-order equation at various temperatures. Vertical bars represent  $\pm 1$  standard deviation ( $n = 3$ ).

1-MCP, which can meet specific demands for different horticultural products. For example, a single application of 1-MCP can protect the floral organs against ethylene for only just 48–96 h for *Chamelaucium uncinatum* Schauer and *Pelargonium peltatum* L.,<sup>30,39,40</sup> so retreating them with 1-MCP or continuous exposure to 1-MCP is needed to prolong their freshness life. However, it is inconvenient during export handling to retreat with 1-MCP. On the basis of the above experiments, the 1-MCP/CB[6] inclusion complex as a sustained release delivery system of 1-MCP in water may contribute to the continuous exposure to 1-MCP problem.

In conclusion, 1-MCP can be encapsulated by CB[6] successfully. The inclusion ratio of 1-MCP/CB[6] was calculated from the TG data as 4.5%, which is similar to that of 1-MCP/ $\alpha$ -CD. CB[6] can be prepared from cheaper starting materials, glycoluril and formalin, than  $\alpha$ -CD. Moreover, the controlled release of 1-MCP could be easily realized for 1-MCP/CB[6] by changing

Table 1. Kinetic Parameters for 1-MCP Adsorption by CB[6]<sup>a</sup>

		T		
		288 K	293 K	298 K
experimental	$Q_e$ (mg/g)	48.7 ± 1.5 c	45.6 ± 0.4 b	40.7 ± 1.1 a
pseudo-first-order model	$k_1$ (min <sup>-1</sup> )	0.014 ± 0.001 a	0.015 ± 0.001 a	0.013 ± 0.001 a
	$R^2$	0.924 ± 0.074 a	0.986 ± 0.004 a	0.958 ± 0.028 a
	$Q_e$ (mg/g)	47.53 ± 1.06 a	65.61 ± 0.86 b	46.75 ± 0.96 a
pseudo-second-order model	$k_2 \times 10^{-3}$ (min <sup>-1</sup> )	0.19 ± 0.02 c	0.05 ± 0 a	0.12 ± 0.01 b
	$R^2$	0.883 ± 0.053 c	0.453 ± 0.091 a	0.685 ± 0.066 b
	$Q_e$ (mg/g)	61.35 ± 1.18 b	81.90 ± 0.82 c	57.04 ± 0.63 a

<sup>a</sup> Values represent the mean ± SD. Values labeled with the same letter within the same row are not significantly different at the 5% level, applying Tukey's test.

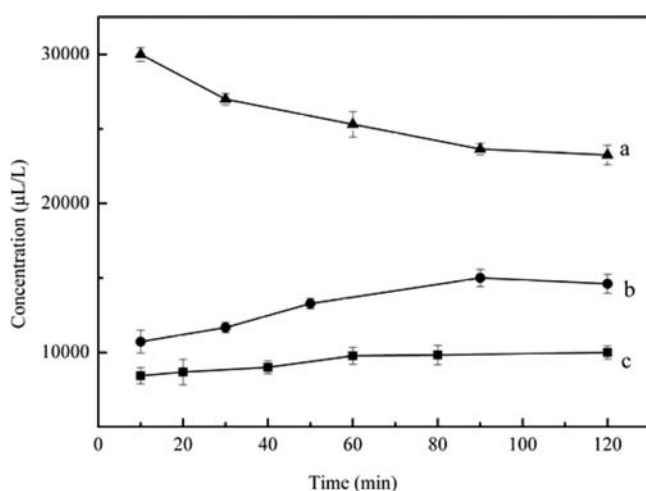


**Figure 11.** Release of 1-MCP from complex in sodium bicarbonate (a), benzoic (b), and distilled water (c) media. 1-MCP was produced by injection of 1 mL of a 3% solution into 0.1 g of inclusion complex in a 25 mL vial. Vertical bars represent ± 1 standard deviation ( $n = 3$ ).

the pH of the releasing solution. Therefore, the application of 1-MCP/CB[6] in the horticultural product has a promising future and deserves further attention.

## AUTHOR INFORMATION

### Corresponding Author

\*E-mail: jianghong0066@126.com.

### Funding Sources

The present work was supported by the Fundamental Research Funds for the Central Universities (Program 2011PY088).

## REFERENCES

- (1) Abeles, F. B.; Morgan, P. W.; Saltveit, M. E. *Ethylene in Plant Biology*; Academic Press: San Diego, CA, 1992.
- (2) Watkins, C. B. Ethylene synthesis, mode of action, consequences and control. In *Fruit Quality and Its Biological Basis*; Knee, M., Ed.; Sheffield Academic Press: Boca Raton, FL, 2002; pp 180–224.
- (3) EPA (Environmental Protection Agency). *Fed. Regist.* **2002**, *67*, 796–800.

(4) Serek, M.; Sisler, E. C.; Reid, M. S. Effects of 1-MCP on the vase life and ethylene response of cut flowers. *Plant Growth Regul.* **1995**, *16*, 93–97.

(5) Sisler, E. C.; Serek, M.; Dupille, E. Comparison of cyclopropene, 1-methylcyclopropene, and 3,3-dimethylcyclopropene as ethylene antagonists in plants. *Plant Growth Regul.* **1996**, *18*, 169–174.

(6) Feng, X. Q.; Apelbaum, A.; Sisler, E. C.; Goren, R. Control of ethylene activity in various plant systems by structural analogues of 1-methylcyclopropene. *Plant Growth Regul.* **2004**, *42*, 29–38.

(7) Watkins, C. B. The use of 1-methylcyclopropene (1-MCP) on fruits and vegetables. *Biotechnol. Adv.* **2006**, *24*, 389–409.

(8) Blankenship, S. M.; Dole, J. M. 1-Methylcyclopropene: a review. *Postharvest Biol. Technol.* **2003**, *28*, 1–25.

(9) Reid, M. S.; Staby, G. L. A brief history of 1-methylcyclopropene. *HortScience* **2008**, *43*, 83–85.

(10) Watkins, C. B. Overview of 1-methylcyclopropene trials and uses for edible horticultural crops. *HortScience* **2008**, *43*, 86–94.

(11) Daly, J.; Kourelis, B. Synthesis methods, complexes and delivery methods for the safe and convenient storage, transport and application of compounds for inhibiting the ethylene response in plants. U.S. Patent 6017849, 2001.

(12) Gao, R. T. Microcapsuled fruit, vegetable and flower antistaling agent and preparation thereof. Chin. Patent 10089065, 2005.

(13) Sisler, E. C.; Blankenship, S. M. Method of counteracting an ethylene response in plants. U.S. Patent 5518988, 1996.

(14) Basel, R. M.; Kostansek, E. C. Compositions with cyclopropenes and adjuvants. U.S. Patent 20090088323A1, 2009.

(15) Chong, J. A.; Farozic, V. J.; Jacobson, R. M.; Snyder, B. A.; Stephens, R. W.; Mosley, D. W. Continuous process for the preparation of encapsulated cyclopropenes. U.S. Patent 20020043730A1, 2002.

(16) Jacobson, R. M.; Wehemyer, F. L. Humidity activated delivery systems for cyclopropenes. Eur. Patent 1593306A2, 2005.

(17) Day, A. I.; Blanch, R. J.; Arnold, A. P.; Lorenzo, S.; Lewis, G. R.; Dance, I. A cucurbituril-based gyroscane: a new supramolecular form. *Angew. Chem., Int. Ed.* **2002**, *41*, 275–277.

(18) Freeman, W. A.; Mock, W. L.; Shih, N. Y. Cucurbituril. *J. Am. Chem. Soc.* **1981**, *103*, 7367–7368.

(19) Kim, J.; Jung, I. S.; Kim, S. Y.; Lee, T.; Kang, J. K.; Sakamoto, S.; Yamaguchi, K.; Kim, K. New cucurbituril homologues: syntheses, isolation, characterization, and X-ray crystal structures of cucurbit[ $n$ ]uril ( $n = 5, 7$ , and 8). *J. Am. Chem. Soc.* **2000**, *122*, 540–541.

(20) Day, A.; Arnold, A. P.; Blanch, R. J.; Snushall, B. Controlling factors in the synthesis of cucurbituril and its homologues. *J. Org. Chem.* **2001**, *66*, 8094–8100.

(21) Jeon, W. S.; Moon, K.; Park, S. H.; Chun, H. Complexation of ferrocene derivatives by the cucurbit[7]uril host: a comparative study of the cucurbituril and cyclodextrin host families. *J. Am. Chem. Soc.* **2005**, *127*, 12984–12989.

(22) Leclercq, L.; Noujeim, N.; Sanon, S. H.; Schmitzer, A. R. Study of the supramolecular cooperativity in the multirecognition mechanism of cyclodextrins/cucurbituril/disubstituted diimidazolium bromides. *J. Phys. Chem. B* **2008**, *112*, 14176–14184.

(23) Buschmann, H. J.; Cleve, E.; Mutihac, L.; Schollmeyer, E. A novel experimental method for the study of complex formation between  $\alpha$ -,  $\beta$ - and  $\gamma$ -cyclodextrin and nearly insoluble cucurbituril-[2] rotaxanes in aqueous solution. *Microchem. J.* **2000**, *64*, 99–103.

(24) Zhang, H.; Ferrell, T. A.; Asplund, M. C.; Dearden, D. V. Molecular beads on a charged molecular string:  $\alpha,\omega$ -alkyldiammonium complexes of cucurbit[6]uril in the gas phase. *Int. J. Mass Spectrom.* **2007**, *265*, 187–196.

(25) Buschmann, H. J.; Mutihac, L.; Mutihac, R. C.; Schollmeyer, E. Complexation behavior of cucurbit[6]uril with short polypeptides. *Thermochim. Acta* **2005**, *430*, 79–82.

(26) Liu, L.; Nouvel, N.; Scherman, O. A. Controlled catch and release of small molecules with cucurbit[6]uril via a kinetic trap. *Chem. Commun.* **2009**, *22*, 3243–3245.

(27) Cui, L.; Gadde, S.; Li, W.; Kaifer, A. E. Electrochemistry of the inclusion complexes formed between the cucurbit[7]uril host and several cationic and neutral ferrocene derivatives. *Langmuir* **2009**, *25*, 13763–13769.

(28) Kellersberger, K. A.; Anderson, J. D.; Ward, S. M.; Krakowiak, K. T.; Dearden, D. V. Encapsulation of  $N_2$ ,  $O_2$ , methanol, or acetonitrile by decamethylcucurbit[5]uril ( $NH_4^+$ )<sub>2</sub> complexes in the gas phase: influence of the guest on “lid” tightness. *J. Am. Chem. Soc.* **2001**, *123*, 11316–11317.

(29) Jon, S. Y.; Selvapalam, N.; Kang, J. K.; Kim, S. Y.; Jeon, Y. J.; Lee, J. W.; Kim, K. Facile synthesis of cucurbit[*n*]uril derivatives via direct functionalization: expanding utilization of cucurbit[*n*]uril. *J. Am. Chem. Soc.* **2003**, *125*, 10186–10187.

(30) Fisher, F.; Applequist, D. E. Synthesis of 1-methylcyclopropene. *J. Org. Chem.* **1965**, *30*, 2089–2090.

(31) Magid, R. M.; Clarke, T. C.; Duncan, C. D. Efficient and convenient synthesis of 1-methylcyclopropene. *J. Org. Chem.* **1971**, *36*, 1320–1321.

(32) Wang, X. S.; Tang, Y. P.; Tao, S. R. Kinetics, equilibrium and thermodynamic study on removal of Cr(VI) from aqueous solutions using low-cost adsorbent alligator weed. *Chem. Eng. J.* **2009**, *148*, 217–225.

(33) Gerasko, O. A.; Mainicheva, E. A.; Naumova, M. I.; Yurjeva, O. P.; Alberola, A.; Vicent, C.; Llusar, R.; Fedin, V. P. Tetranuclear lanthanide aqua hydroxo complexes with macrocyclic ligand cucurbit[6]uril. *Eur. J. Inorg. Chem.* **2008**, *3*, 416–424.

(34) Hou, Z. S.; Tan, Y. B.; Zhou, Q. F. Side-chain pseudopolyrotaxanes by threading cucurbituril[6] onto quaternized poly-4-vinylpyridine derivative: synthesis and properties. *Polymer* **2006**, *47*, 5267–5274.

(35) Silverstein, R. M.; Webster, F. X.; Kiemle, D. Infrared spectroscopy. In *Spectrometric Identification of Organic Compounds*, 7th ed.; Debbie, B., Jennifer, Y., Sarah, W. R., Sarah, R., Eds.; Wiley: New York, 2005; p85.

(36) Lim, S.; Kim, H.; Selvapalam, N.; Kim, K. J.; Cho, S. J.; Seo, G.; Kim, K. Cucurbit[6]uril: organic molecular porous material with permanent porosity, exceptional stability, and acetylene sorption properties. *Angew. Chem., Int. Ed.* **2008**, *47*, 3352–3355.

(37) Li, C. F.; Dua, L. M.; Zhang, H. M. Study on the inclusion interaction of cucurbit[*n*]urils with sanguinarine by spectrofluorimetry and its analytical application. *Spectrochim. Acta A* **2010**, *75*, 912–917.

(38) Michael, C. P.; Anthony, B. B.; Yoshihisa, I.; Fernando, I. R.; Norimitsu, S.; Takehiko, W.; Zou, Y. F.; Brad, M. B. Ethylene receptor antagonists: strained alkenes are necessary but not sufficient. *Chem. Biol.* **2008**, *15*, 313–321.

(39) Cameron, A. C.; Reid, M. S. 1-MCP blocks ethylene-induced petal abscission of *Pelargonium peltatum* but the effect is transient. *Postharvest Biol. Technol.* **2001**, *22*, 169–177.

(40) Macnish, A. J.; Joyce, D. C.; Hofman, P. J.; Simons, D. H.; Reid, M. S. 1-Methylcyclopropene treatment efficacy in preventing ethylene perception in banana fruit and grevillea and waxflower flowers. *Aust. J. Exp. Agric.* **2000**, *40*, 471–481.